



## Ecofriendly biosorption of atrazine herbicide in aqueous solution by *Moringa oleifera* Lam: kinetics, equilibrium and thermodynamics

Priscila Ferri Coldebella<sup>a</sup>, Marcia Regina Fagundes-Klen<sup>b</sup>, Driano Rezende<sup>a</sup>,  
Aline Takaoka Alves Baptista<sup>c</sup>, Leticia Nishi<sup>a</sup>, Quelen Leticia Shimabuku<sup>b</sup>,  
Rosângela Bergamasco<sup>a,c,\*</sup>

<sup>a</sup>Programa de Pós-Graduação em Engenharia Química, Universidade Estadual de Maringá, Avenida Colombo 5790, CEP 87020-900, Maringá-PR, Tel. +55 44 3011 4782; emails: rbergamasco@uem.br (R. Bergamasco), pricoldebella@gmail.com (P.F. Coldebella), drirezend@gmail.com (D. Rezende), leticianishi@hotmail.com (L. Nishi)

<sup>b</sup>Departamento de Engenharia Química, Universidade Estadual do Oeste do Paraná, Rua da Faculdade 645, CEP 85903-000, Toledo, Paraná, Brazil; emails: fagundes.klen@gmail.com (M.R. Fagundes-Klen), le.shimabuku@gmail.com (Q.L. Shimabuku)

<sup>c</sup>Departamento de Engenharia Química, Universidade Estadual de Maringá, Avenida Colombo 5790, CEP 87020-900, Maringá-PR, Tel. +55 44 3011 4782; email: alinetakaoka\_17@hotmail.com (A.T.A. Baptista)

Received 24 January 2018; Accepted 3 August 2018

### ABSTRACT

The water contamination by herbicides, such as atrazine, causes negative impacts, affecting animal's and human's health. The *Moringa oleifera* Lam seed is proposed as a material for atrazine biosorption from water. The initial atrazine concentration was 5 mg L<sup>-1</sup>, the adsorption assays showed that the relevant parameters to the process were the effect of pH and the adsorbent mass. Models of pseudo first order and pseudo second order and intraparticle dissemination were applied in the experimental results. The kinetic model of first-order Lagergren (pseudo) explained the experimental adsorption results; the kinetic equilibrium was reached in 20 minutes, and atrazine removal was 76%. The maximum sorption capacity was calculated to the Langmuir (0.653 mg g<sup>-1</sup>) and Freundlich (0.125 mg g<sup>-1</sup> L<sup>1/n</sup> mg<sup>-1/n</sup>) isotherms models. The thermodynamic parameters  $\Delta G^\circ$  (kJ mol<sup>-1</sup>),  $\Delta H$  (kJ mol<sup>-1</sup>), and  $\Delta S$  (kJ mol<sup>-1</sup>K<sup>-1</sup>) (Gibbs free energy, enthalpy, and entropy), showed negatives values, such as -3.98 to -5.09, -21.76, and -0.056, respectively. The interaction of functional atrazine groups with the adsorbent surface was confirmed by Fourier-transform infrared spectroscopy analysis. As the seed is a complex and heterogeneous biomass, it is suggested that the Freundlich model is more appropriate to explain how the atrazine biosorption occurs.

**Keywords:** Atrazine; Adsorption; *Moringa oleifera*; Water treatment

### 1. Introduction

The use of pesticides in the world has increased during the last decades with the change of practice and increase of intensive agriculture. This widespread use of pesticides for agricultural and non-agricultural purposes resulted in the presence of pesticide residues in environmental matrices.

Pesticides are relatively stable, and bioaccumulation may occur in different organisms [1–4].

Atrazine (ATZ) was selected as a pollutant target, because it belongs to the large group of pesticides. The ATZ carcinogenic and endocrine disruptor nature has led many countries to prohibit or restrict its use [5]. Despite its restricted use, ATZ was detected in aqueous environments above its maximum permissible level in several countries [6,7].

\* Corresponding author.

To keep humans and other animals safe from toxic and harmful effects of ATZ and other pesticides, this pesticide have to be removed or reduced from soil and water [8]. Several studies of water treatment, including advanced oxidation processes, electrocoagulation, and membrane techniques have been developed. One of the most widely used methods for removing these dangerous substances from polluted water is the adsorption. The adsorption studies have been centered in the evaluation of alternative adsorbents, that is, low-cost adsorbents, including the use of residues (industrial and agricultural residues) capable of removing significant quantities of various pollutants from aqueous solutions [2].

Plant material can be considered as a heterogeneous material containing a lot of binding sites, resembling a chromatographic system with partition (absorption) and adsorption chromatography in varied polarity supports. Thus, it seems appropriate to use seeds or oil-containing agricultural by-products as biosorbents for ATZ elimination from aqueous environments [9].

The *Moringa oleifera* (MO) seeds are distinguished by their coagulant ability, playing an important role in the search for alternative water treatments. Many studies have been developed on the use of MO seeds (pulp) for water purification, because the seeds have cationic polyelectrolytes with proven efficacy in the water treatment replacing the aluminum sulfate.

Biosorption is a promising alternative to replace or complement the processes for organic pollutants removal from water and wastewater [10,11]. For inactive biomass, the adsorption mechanism can depend on the chemical pollutant nature (size, ionic charge), type of biomass, its preparation, and properties of specific surface (particle size, functional groups), process conditions (pH, temperature, agitation, presence of organic, or inorganic groups in the solution), and maximum adsorption capacity (adsorbent dose, contact time, and initial concentration) [12,13].

This work has an objective to investigate the biosorption potential of the MO seed for ATZ removal in aqueous solution. Therefore, the adsorption conditions were statistically evaluated (particle size, pH, temperature, agitation speed, biosorbent dosage, and initial ATZ concentration). In addition, kinetic study and thermodynamic equilibrium of the biosorption process were performed. This study will lead to a better understanding of the biosorption process and will demonstrate its possible usefulness for organic contaminants removal from aqueous solution.

## 2. Material and methods

The experimental studies of biosorption are represented in Fig. 1.

### 2.1. Reagents and materials

The reagents used in this work were purchased from Sigma-Aldrich Co., USA or J.T. Baker® Chemicals, USA. Reference standard of ATZ with purity of 98.8% was purchased from Fluka® Analytical by Sigma-Aldrich Co., USA (Ref. 90935). This analytical standard was used for the calibration curve preparation in high-performance liquid

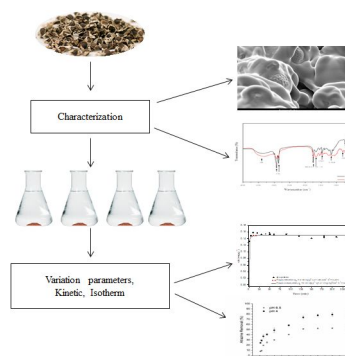


Fig. 1. Scheme of experimental biosorption studies of atrazine and *Moringa* seeds.

chromatography (HPLC) analysis. Methanol (HPLC grade 99.9%), was purchased from J.T. Baker® and used for making synthetic aqueous solutions and for HPLC method [14].

### 2.2. Preparation of synthetic ATZ solution

Synthetic water, with 0.1–20 mg L<sup>-1</sup> of ATZ, was prepared from the commercial product of 500 g L<sup>-1</sup> of ATZ (500 SC Nortox, Brazil) and of ultrapure water system (Milli-Q®, Millipore, USA). The solution pH of synthetic ATZ solution for the experiment was 6.5.

### 2.3. Determination of ATZ by HPLC

ATZ was analyzed through HPLC using an Agilent Varian 920 LC chromatograph (Mulgrave, Australia) equipped with an auto sampler, a quaternary gradient pump, and a diode array detector equipped with a Galaxie™ Chromatography Software. The calibration curve was prepared from 0.05 to 20 mg L<sup>-1</sup> of standard ATZ (Fluka® Analytical, USA) in methanol (J.T. Baker®). The HPLC conditions were as follows: ODS C18 column (5 μm, 25 cm × 4.6 mm, Phenomenex), mobile phase (65% methanol: 35% ultrapure water), flow rate (0.8 mL min<sup>-1</sup>), detection (222 nm) at 5.1 min. A detection limit of 0.01 mg L<sup>-1</sup> was obtained by Coldebella et al. [14].

The samples were filtered in cellulose acetate filter (Millipore), 0.45 μm of porosity, before HPLC analysis.

### 2.4. Preparation and characterization of MO seeds

The parts of MO, barks and seeds (pulp), were separated. The seeds were dried in an oven with air circulation (Digital timer SX CR/42) at 40°C until constant weight [15]. Then, the husks were dried at 60°C for 24 h, ground in a commercial blender and particle size separated using a sieve shaker (Bertel, Brasil) with different sizes of mesh, 150–700 μm. The MO seeds were characterized by determination of the zero point of charge (pH<sub>pCZ</sub>), Fourier-transform infrared spectroscopy (FTIR), and scanning electron microscopy (SEM). pH<sub>pCZ</sub> was determined following the method described by Regalbuto and Robles [16] and measured in pH meter (Orion™ Versa Star Benchtop Meter, Thermo Scientific™, USA). The presence of functional groups in the MO seeds was characterized before and after the biosorption process, using FTIR 100 Spectrum in the range from 4,000 to 400 cm<sup>-1</sup>. In the morphological

characteristic evaluation of the MO seeds, a scanning electron microscope SS 550 Superscan was used.

### 2.5. Biosorption experiments with ATZ solutions

For the ATZ biosorption experiments, the following parameters were used: particle size, agitation speed, pH, temperature, and adsorbent mass. Batch adsorption experiments were performed setting a volume of 25 mL solution and initial ATZ concentration of 5 mg L<sup>-1</sup>. The temperature and agitation were controlled in incubator (Tecnal TE-4200) with orbital shaking. The samples were collected and filtered in cellulose acetate filter of 0.45 µm and analyzed by HPLC for ATZ concentration in different times.

#### 2.5.1. Effect of particle size

The ATZ adsorption was studied for different particle sizes of MO seeds. The evaluated sizes were 100, 150, 300, 500, and 700 µm and total (approximately 8.000 µm). The batch experiment was carried out fixing the mass of adsorbent of 0.1 g, temperature of 25°C ± 2°C, pH 6.5, agitation speed of 100 rpm, and contact time of 60 min.

#### 2.5.2. Effect of shaking speed

The shaking speed varied in 100, 150, and 200 rpm. The batch experiments were performed by fixing the size of adsorbent particle at 500 µm, mass of adsorbent of 0.1 g, temperature of 25°C ± 2°C, pH 6.5, and contact time of 60 min.

#### 2.5.3. Temperature effect

The temperature effect on the ATZ biosorption by MO seed was monitored by varying the temperature at 25°C, 35°C, and 45°C. Therefore, the experiment was carried out fixing the size of the adsorbent particle at 500 µm, mass of adsorbent of 0.1 g, pH 6.5, agitation speed of 100 rpm, and contact time of 60 min.

#### 2.5.4. pH effect

The initial pH of the ATZ solutions was adjusted into 2, 3, 4, 5, 6, 7, 8, 9, and 10 with solutions of HCl and NaOH 0.1 mol L<sup>-1</sup>. The batch experiments were performed by fixing the size of adsorbent particle at 500 µm, mass of adsorbent of 0.1 g, temperature of 25°C ± 2°C, agitation speed of 100 rpm, and contact time of 60 min. The pH analysis at the end of the experiment was also performed.

#### 2.5.5. The mass of adsorbent effect

To evaluate the effect of adsorbent mass, the MO seed mass ranged from 0.01 to 1.2 g. The MO seeds dosages in size of 500 µm were placed in contact with aqueous ATZ solution corrected at pH 4 and 6.5, at a temperature of 25°C ± 2°C, shaking speed of 100 rpm during 60 min.

#### 2.5.6. Data analysis

To evaluate the effect of the parameters studied, the ATZ removal efficiency was calculated [17]:

$$\text{Atrazine removal (\%)} = \frac{(C_i - C_{eq})}{C_i} \times 100 \quad (1)$$

where  $C_i$  is the initial ATZ concentration in solution (mg L<sup>-1</sup>) and  $C_{eq}$  is the ATZ concentration in equilibrium (mg L<sup>-1</sup>).

The parameter effects significance was verified by analysis of variance (ANOVA) and Tukey test, with 95% of confidence, being significant  $p$ -value < 0.05, using the statistical program Statistica version 8.0. The experiments were performed with three repetitions.

### 2.6. Kinetic study

The best results obtained by the parameters variation that can directly influence the ATZ biosorption by MO seed were used in the kinetic study of the adsorption process. For that an experiment was carried out using 25 mL of ATZ solution, with concentration of 5 mg L<sup>-1</sup>, particle size of 500 µm, adsorbent mass of 0.6 g, temperature at 25°C ± 2°C, pH 4 ± 0.2, and agitation speed at 100 rpm. The samples were collected in pre-determined intervals of time (2–240 min), 0.45 µm membrane filtered and analyzed by HPLC. The adsorption capacity ( $q_{eq}$ ) was determined by Eq. (2).

$$q_{eq} = \frac{(C_i - C_{eq})}{m} \times V \quad (2)$$

where  $q_{eq}$  is the adsorption capacity of ATZ in equilibrium (mg g<sup>-1</sup>),  $V$  is the solution volume (L),  $C_i$  is the initial concentration of ATZ in the solution (mg L<sup>-1</sup>),  $C_{eq}$  is the ATZ concentration in equilibrium (mg L<sup>-1</sup>), and  $m$  is the mass of adsorbent (g).

In order to investigate the biosorption mechanism, the constants of ATZ biosorption, and intraparticle diffusion, the experimental data were adjusted in the pseudo-first-order model proposed by Lagergren [18] and pseudo-second-order model [19].

The pseudo-first-order model is presented in Eq. (3):

$$q_t = q_{eq} \times (1 - e^{-k_1 t}) \quad (3)$$

where  $q_t$  is the ATZ concentration in the solid phase at time  $t$  (mg g<sup>-1</sup>),  $q_{eq}$  is the adsorption capacity of ATZ in equilibrium (mg g<sup>-1</sup>), and  $k_1$  is the constant rate of adsorption of the pseudo-first-order model (min<sup>-1</sup>).

The pseudo-second-order model is shown in Eq. (4) [19]:

$$q_t = \frac{k_2 \times q_{eq}^2 \times t}{1 + k_2 \times q_{eq} \times t} \quad (4)$$

where  $k_2$  is a constant rate of adsorption of the pseudo-second-order model (g mg<sup>-1</sup> min<sup>-1</sup>).

2.7. Adsorption isotherms

To determine the equilibrium data, the ATZ concentration varied from 0.1 to 20 mg L<sup>-1</sup> solution and the temperature from 25°C to 45°C. The batch experiment was carried out fixing the particle size of the adsorbent at 500 μm, mass of adsorbent at 0.6 g, pH 4, agitation speed at 100 rpm, and contact time at 60 min.

The collected samples were filtered and analyzed by HPLC. Models described by Langmuir and Freundlich were used which describe the non-linear equilibrium between the organic pollutant adsorbed on the adsorbent surface ( $q_{eq}$ ) and the organic pollutant in solution ( $C_{eq}$ ) at a constant temperature.

The Langmuir [20] model is shown in Eq. (5):

$$q_{eq} = \frac{q_{max} b_L C_{eq}}{1 + b_L C_{eq}} \tag{5}$$

where  $q_{max}$  is the maximum adsorption capacity (mg g<sup>-1</sup>) and  $b_L$  is the constant of equilibrium of Langmuir (L mg<sup>-1</sup>) related to the adsorption energy.

The essential isotherm characteristic can be expressed by the dimensionless constant named parameter of equilibrium ( $R_L$ ), given by Eq. (6):

$$R_L = \frac{1}{1 + b_L \cdot C_i} \tag{6}$$

where  $C_i$  is the highest initial concentration (mg L<sup>-1</sup>). If  $0 < R_L < 1$ , the adsorption is favorable.

The mathematical model described by Freundlich [21] is shown in Eq. (7):

$$q_{eq} = k_F (C_{eq})^{n_F} \tag{7}$$

where,  $k_F$  and  $n_F$  are the Freundlich constants on the adsorption capacity in multilayers and adsorption intensity. If the value of  $n_F$  is lower than 1, the adsorption is considered favorable.

2.8. Adsorption thermodynamics

According to the dependence on the structure and surface, functional biosorbent groups, the temperature has an impact on the adsorption capacity. The change of free energy of Gibbs ( $\Delta G^\circ$ ), enthalpy ( $\Delta H$ ), and variation of entropy ( $\Delta S$ ) is very important thermodynamic parameters of adsorption which can confirm the viability, spontaneity, and heat change for the biosorption process [2]. The free energy of Gibbs ( $\Delta G^\circ$ ) was calculated by Eq. (8) for the temperature monitored in the ATZ biosorption study.

$$\Delta G^\circ = -R.T.\ln k_d \tag{8}$$

where,  $R$  is the universal constant of gases (8.314 J mol<sup>-1</sup> K<sup>-1</sup>),  $T$  is the temperature in Kelvin (K), and  $K_d$  is the distribution coefficient. The value of  $K_d$  was calculated using Eq. (9) [22]:

$$K_d = \frac{q_e}{C_e} \tag{9}$$

where  $q_e$  and  $C_e$  are the sorbate equilibrium concentrations in the biosorbent (mg L<sup>-1</sup>) and in the solution (mg L<sup>-1</sup>), respectively.

It should be noted that this simplification is only valid for dilute solutions and neutral or weak-charged species (e.g., organic compounds, such as dyes molecules) [23,24].

The enthalpy and the entropy were estimated through the van't Hoff equation:

$$\ln K_d = \frac{\Delta S}{R} - \frac{\Delta H}{RT} \tag{10}$$

where  $\Delta H$  and  $\Delta S$  were obtained through the angular and linear coefficient of the graphic obtained between  $\ln K_d$  vs.  $1/T$ , respectively.

3. Results and discussion

3.1. Characterization of the MO seed

The  $pH_{PCZ}$  of materials indicates that the particles charge behavior of the biomaterial surface, where the pH value is determined where the surface loads nullify themselves. Fig. 2 presents the  $pH_{PCZ}$  analysis of the MO seed.

When analyzing the  $pH_{PCZ}$  of biomass as a function of pH (Fig. 2), it was found that the region of neutral electrical zone for the MO seed is between pH 4 and 9. The exact  $pH_{PCZ}$  is the pH value when the variation  $\Delta pH$  (initial pH-final pH) is zero (pH where the curve intersects the x-axis). Thus, the value of  $pH_{PCZ}$  was 5.35 for seed.

Therefore, depending on the pH solution, the MO seeds surfaces can be loaded positively or negatively. For pH values greater than  $pH_{PCZ}$ , the surface biomass is negatively charged, which favors the cationic species adsorption. However, the adsorption of anion species will be favored at  $pH < pH_{PCZ}$ . The  $pH_{PCZ}$  of the MO seeds were also found by Alves et al. [25] and Araújo et al. [26], indicating that the biosorbent surface is acidic.

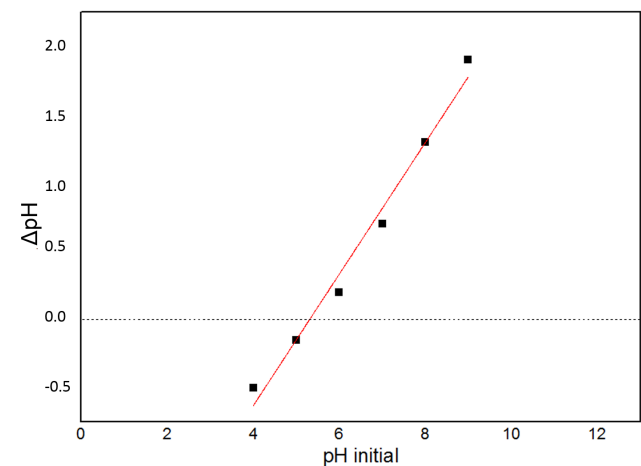


Fig. 2.  $pH_{PCZ}$  analysis of *Moringa oleifera* Lam seed.

This surface charge variation of the biosorbent caused by protonation and deprotonation is reflected by the presence of functional groups that are shown in Fig. 3. The MO seed is composed of a complex matrix, rich in groups of amino acids (proteins), fatty acids, and carbohydrates that may serve as interaction sites for ATZ adsorption.

When comparing the FTIR spectra of the MO seed before and after the ATZ adsorption, it can be observed that a change has occurred between the regions of 500 and 1,400  $\text{cm}^{-1}$ , region which highlights bonds deformations  $\pi$ ,  $\text{C}=\text{C}=775\text{ cm}^{-1}$  and  $\text{C}-\text{H}$  or  $=\text{CH}_2$ , that is, unsaturated carbons terminals, between 830 and 930  $\text{cm}^{-1}$  [27,28]. In 1,163  $\text{cm}^{-1}$ , there was an increase in the signal to the MO seed after adsorption due to vibration of the alcohols groups, phenols, and carboxylic elongation [29]. In 840  $\text{cm}^{-1}$ , the weak signal present in the MO seed before the adsorption is due to the presence of sulfur group [30]. There was the emergence of a weak signal of bond  $\text{C}-\text{Cl}$  in 724  $\text{cm}^{-1}$  in the MO seed after the ATZ adsorption, due to its constitution there is the presence of Cl.

The functional groups  $\text{COOH}^-$ ,  $\text{OH}^-$ , or  $\text{C}=\text{O}^-$  found, are nucleophilic radicals of organic molecules present in the MO seed that can interact with ATZ. These groups are easily ionizable that can interact by electrostatic interaction or Van der Waals forces. ATZ in acids pH also tends to decouple being protonated and may improve its adsorption.

To evaluate the differences in the MO samples composition before and after the ATZ adsorption, the areas relating to integrated absorbance are presented in Table 1

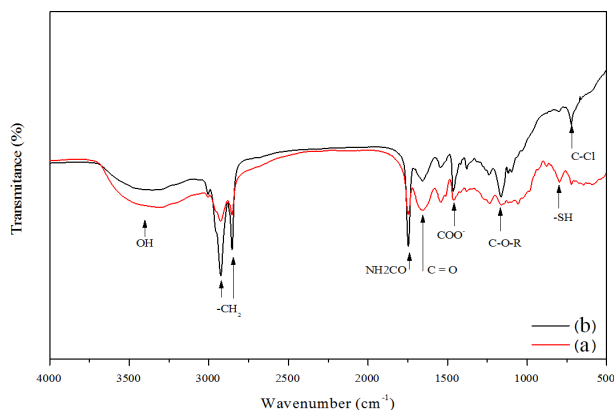


Fig. 3. Spectrum of  $\text{pH}_{\text{PCZ}}$  of *Moringa oleifera* Lam seed (a) before atrazine adsorption and (b) after the atrazine adsorption.

Table 1

The number of wave band, functional group to which is related to, and integrated area of relative absorption to the *Moringa oleifera* Lam seed before and after atrazine adsorption

Number of wave ( $\text{cm}^{-1}$ )	Functional group	$A_{\text{peak}}/A_{\text{total}}$ seed	$A_{\text{peak}}/A_{\text{total}}$ seed after adsorption
3,380	$-\text{OH}$	0.287	0.178
2,925/2,850	$-\text{CH}$ aliphatic	0.044	0.130
1,745	$-\text{RNHCO}$	0.021	0.051
1,650	$-\text{C}=\text{O}$	0.040	0.030
1,464	$-\text{COO}^-$	0.019	0.030

(peak area/total area) of bonds  $\text{O}-\text{H}$ ,  $\text{C}-\text{H}$ ,  $\text{C}=\text{O}$ , and  $\text{COOH}$ .

In Table 1, the areas of the most relevant peaks of functional groups in the spectrum were calculated by mathematical method of polygonal area [31]. It could be observed that the sample after adsorption presented lower content of OH groups due to the numerous compounds present in the seed solubilized in water. There was an increase in fat content bonds  $\text{CH}$ ,  $\text{CNH}$ ,  $\text{C}=\text{O}$ , and  $\text{COO}^-$ , by the ATZ molecule adsorption. It is believed that there may be bonds of hydrogen bridges between the grouping of secondary amine molecule of ATZ and the groups  $\text{OH}$  or  $\text{C}=\text{O}$  of the adsorbent. This type of interaction occurred in several studies of ATZ sorption in organic matter present in the soil [32].

Another way of ATZ interacting with the MO surface is by electrostatic forces, as shown by the  $\text{pH}_{\text{PCZ}}$  analysis, the surface has acidic traits and some functional groups, such as carboxylic acids, above pH 4, can be dissociated in their combined base, that is, carboxylates ions ( $\text{R}-\text{COO}^-$ ) [33]. On the other hand, according to Weber [34], the ATZ in acidic conditions can receive  $\text{H}^+$ , protonating amine groups present in the molecule, especially in nitrogens present in triazine ring ( $\text{N}=\text{NH}^+$ ), which are more easily ionizable (at pH values lower than 5). Therefore, in a broad range of pH conditions for this system, there will be an interaction of loads between the MO surface and the ATZ molecules. However, while the pH values become more acidic, the carboxylic groups, as well as other clusters on the adsorbent surface, turn out to having cationic characteristic, thus leading to the electrostatic repulsion between the adsorbent and triazine (see results of adsorption as a function of pH—Fig. 5).

According to Ali et al. [1], the main physical forces acting in the adsorption process are Van der Waals forces, hydrophobic interaction, hydrogen bonds, steric interaction and through polarity, induced dipole interactions, interaction of type  $\pi-\pi$ , etc. Considering the heterogeneous characteristics of the MO structure due to the composition of the lignocellulosic complex, as observed in the results of FTIR (see Fig. 3), it is very likely that several intermolecular interactions can occur simultaneously. It should be emphasized that the intensity and the existence of such forces are dependent on the process operating conditions.

Figs. 4(a) and (b) are the SEM of the MO seed before and after the ATZ adsorption.

In Fig. 4(a), it can be observed that the material presents morphological characteristics distributed with heterogeneity and relatively porous. The presence of deformations on the plant tissue surface, containing available spaces that allow the favorable adsorption conditions, is visible. After the adsorption process, it is observed in Fig. 4(b), the presence of a thin layer on the seed surface, closing the porous protuberance shown in Fig. 4(a).

The biosorbent surface has an important role whatever the involved biosorption mechanism that may be related to the ion exchange capacity, chemical or physical adsorption [35].

### 3.2. ATZ biosorption assays

To evaluate the effects that influenced the adsorption process, the following parameters were studied: particle size, agitation speed, effect of pH, temperature effect, and mass of adsorbent for an ATZ concentration of 5  $\text{mg L}^{-1}$ .

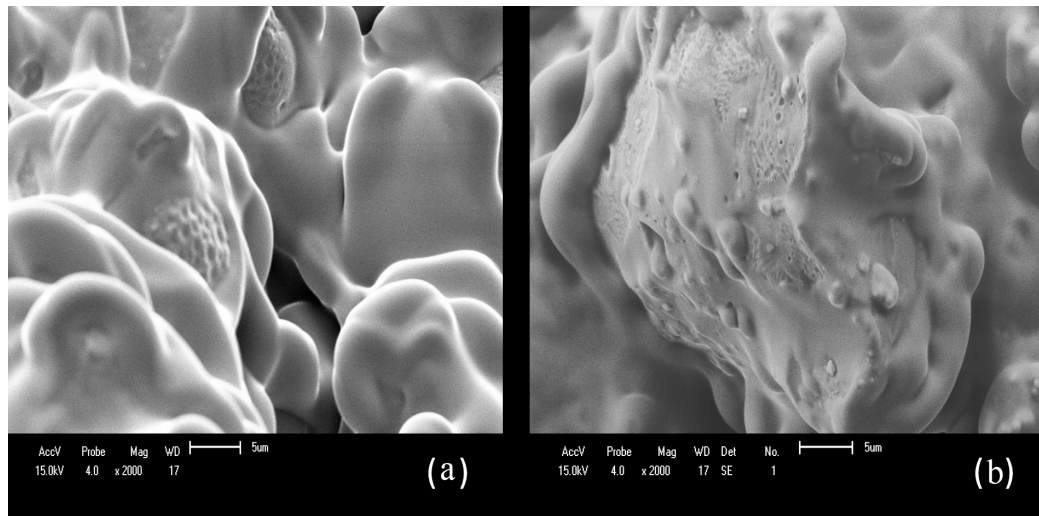


Fig. 4. Scanning electron microscopy of *Moringa oleifera* Lam seed (a) before and (b) after the atrazine adsorption (magnitude 2000X.)

With the experimental data of the removal efficiency, a statistical ANOVA was performed to check which effects were significant in the ATZ biosorption process. The effects were considered significant when  $p$ -value < 0.05 with a confidence level of 95%. In Table 2, the  $p$ -values of ANOVA are shown for the parameters evaluated in the ATZ biosorption process.

It is observed in Table 2 that the parameters that were significant in the adsorption process were the effect of pH and the mass of the adsorbent. The biosorption was not influenced by the particle size, agitation speed, and temperature.

Thus, a particle size of 500 µm was adopted, the same adopted to characterize the adsorbent material; however, crushed seeds could have been used without the need for a separation process. As the increase of agitation speed did not significantly influence on the adsorption, it was chosen to evaluate the kinetics and the adsorption isotherms of the agitation speed of 100 rpm due to lower energy cost. In order to carry out, the kinetic study a temperature of 25°C was adopted; however, this effect will also be assessed when the adsorption isotherms are determined later.

For the studied parameters pH and mass of adsorbent, the means comparison test, Tukey test at 95% confidence intervals were performed, to check where the significant differences of the adsorption tests are.

In Fig. 5, the behavior of ATZ biosorption is demonstrated in different pH values.

Values from 39.3% to 38.46% of ATZ removal efficiency were found between pH 2 and 4, which did not differ statistically. The MO adsorption efficiency was slightly increased with a decrease in pH. This can be attributed to the presence of hydrogen ions at lower pH, resulting in electrostatic interaction between ATZ and the seed surface. While on the contrary, the presence of hydroxyl ions at more elevated pH can result in the ATZ sorption suppression [17,36]. As shown in the FTIR analyses, the MO seeds are rich in proteins, lipids, and crude fiber; therefore in their matrices there are groups of carboxylic acids, carbonyls, and amine, where these functional groups can be decoupled in different values of pH and, consequently, participate of the

Table 2  
Values of  $p$ -value for the efficient atrazine removal using *Moringa oleifera* Lam seed

Variation parameters	$p$
Particle size	0.062**
Agitation speed	0.104**
Temperature effect ( $T$ )	0.175**
pH effect	0.0015*
Adsorbent mass	<0.0001*

\*Significant at a confidence level of 95%.

\*\*Non significant.

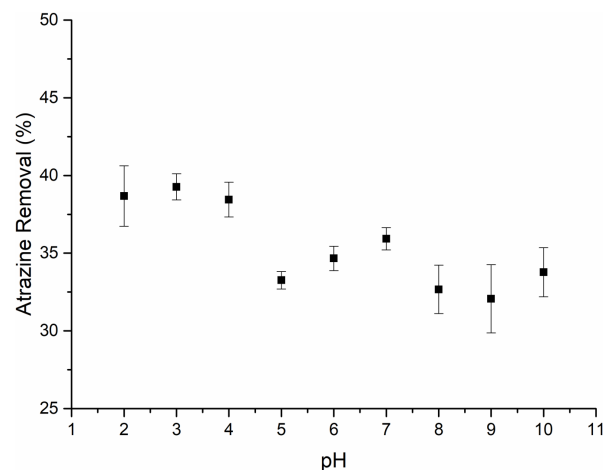


Fig. 5. Influence of pH in the atrazine removal. pH values do not differ among themselves, by the Tukey test at 5% significance level.

biosorption process. Therefore, the adsorption mechanism and, consequently, the ATZ adsorption capacity are significantly influenced by pH.

Thus, based on the adsorption results as a function of pH, as well as the modifications (displacement and variation

in the intensity) of the bands observed by FTIR analysis (especially,  $\text{C}=\text{O}$  and  $\text{COO}^-$ ) (see Table 1), it is possible to say that at pH 4, the electrostatic forces act synergistically with other interactions present as a bridge of hydrogen and Van der Waals forces, in view of the present clusters present in the biosorbent and ATZ. In this pH, therefore, the carboxylic groups are dissociated presenting anionic characteristic ( $\text{pK}_a \approx 3\text{--}5$ ), which is electrostatically attracted by the protonated amides ( $\text{C}=\text{NH}^+$ ) in the same pH value.

The organic species adsorption present in solution in a positive way, will be favored in pH where negative species predominate on the biosorbent surface; however, many species can undergo hydrolysis, hence dissociating and forming metabolites both in the solution medium and on the adsorbent surface, as it is the case of ATZ which is a polar compound and weakly basic [37]. The acidic or alkaline hydrolysis of ATZ produces one of its most abundant degradation products: hydroxy ATZ; its solubility in water is almost independent of the pH solution; however, it increases in solutions whose pH is lower than 2.0 [32]. Thus, in addition to the best removal capabilities, as well as to avoid the occurrence of the by-products formation, it is suggested that the adsorption process occurs at pH 4.

As the effect of pH was significant in the ATZ biosorption, the effect of MO seed mass was studied in two pHs: 4 and 6.5. Through the ANOVA, it was verified that both the pH and the mass of adsorbent are significant. The results are shown in Fig. 6.

ATZ removal ranged from 24% to 80% for pH 4 and from 8% to 53% for pH 6.5 were obtained in this experiment. Through Fig. 6, it was possible to observe that the ATZ removal increases as the mass of adsorbent increases and the

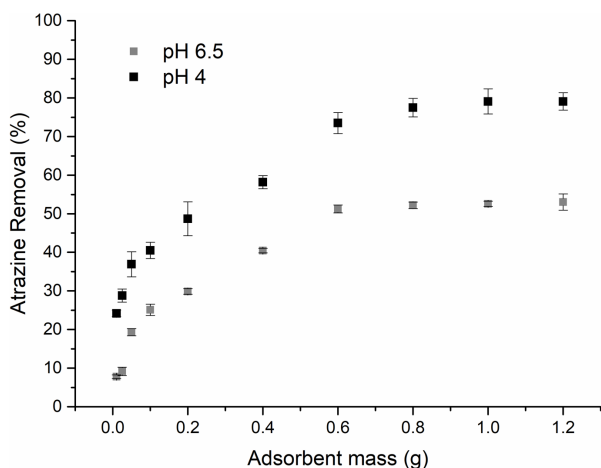


Fig. 6. Adsorbed atrazine removal in function of the MO seeds dosage in 0.01–1.2 g, 5 mg L<sup>-1</sup> of atrazine, 100 rpm at 25°C in pH 4 and 6.5.

Table 3

Constants of the pseudo-first order (Lagergren) and pseudo-second order models (McKay)

Pseudo first order			Pseudo second order		
$k_1$ (min <sup>-1</sup> )	$q_{eq}$ (mg g <sup>-1</sup> )	$R^2$	$k_2$ (g mg <sup>-1</sup> min <sup>-1</sup> )	$q_{eq}$ (mg g <sup>-1</sup> )	$R^2$
1.025	0.151	0.982	31.174	0.151	0.975

pH decreases. For adsorbents mass below 0.6 g, statistical differences were found on the ATZ adsorption in different pHs; however, from 0.6 g of adsorbent to the extent that the system reached the adsorption equilibrium the mass did not influence significantly the amount of adsorbed ATZ. With these results, it can be assumed that doses of 0.6 g of adsorbent are sufficient for ATZ removal to 5 mg L<sup>-1</sup>.

Raghuvanshi et al. [38] observed in their study that the increase in the contaminant removal on the adsorption occurs, probably, due to a high driving interaction force and higher superficial area, occupying the sites available in the adsorbent. Therefore, when the sites are still unsaturated, the removal efficiencies are highest.

Considering the results, it was found that for the ATZ biosorption process, at a concentration of 5 mg L<sup>-1</sup> and a volume of 25 mL, using MO seed through the parameters studied the best conditions were particle size, 500 μm; agitation speed, 100 rpm; temperature, 25°C; pH, 4; and mass of adsorbent, 0.6 g.

From these parameters kinetic studies were performed, obtaining isotherms and energies of the adsorption process.

### 3.3. Kinetic study

The adjustment of the experimental data to kinetic models of pseudo first order and pseudo second order, as well as the parameters obtained from this adjustment, are presented in Fig. 7.

In Fig. 7, it is observed that the adsorption equilibrium was reached after 20 min. The values of the amount of adsorbed ATZ were 0.151 mg g<sup>-1</sup>, for the two models used, agreeing with what was found experimentally,  $q_{eq\text{ experimental}} = 0.150$  mg g<sup>-1</sup>, equivalent to 76% of ATZ removal.

Table 3 exhibits a summary of the kinetic models applied in the ATZ biosorption by MO seed.

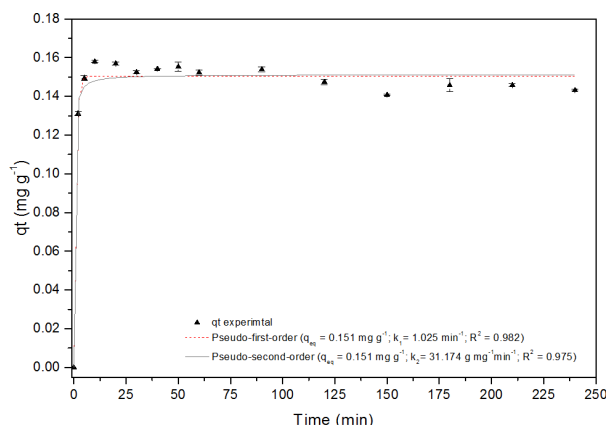


Fig. 7. Adjustment of the experimental data to kinetic models of pseudo first order and pseudo second order.

When the regression coefficients of kinetic models are compared with ATZ, it is observed that they are higher than 0.90.

When the diffusion is fast and occurs within the first 30 min of the adsorption, it can happen for macro and mesoporous adsorbent materials [19], which may be a characteristic of the MO seed

Both the kinetic model of pseudo first order and pseudo second order fit to the experimental data, with a correlation coefficient of 0.982 and 0.975, respectively. However, the model of pseudo first order explained the experimental data better.

This observation clarifies that the biosorption process follows kinetics of pseudo first order, because in the first step of adsorption, diffusion in the film is an important step to control speed and external mass transfer or diffusion boundary layer can be characterized by the initial rate of the solute biosorption [12].

According to Ayranci and Hoda [39], the adsorption of several organic molecules, including some pesticides, on the natural materials surface takes place in a way to follow kinetics of pseudo first order. This same model was used by Akhtar et al. [17] to explain the contaminants biosorption benzene, toluene, ethylbenzene, and cumene using the MO pod.

### 3.4. Adsorption isotherms

The adsorption isotherms models tested were Langmuir and Freundlich isotherm, in order to explain the experimental data obtained in the test of ATZ adsorption equilibrium

by the MO seed, shown in Fig. 8. In the experiment, the ATZ adsorption was evaluated at concentrations ranged from 0.01 to 20 mg L<sup>-1</sup> and a time of 60 min for the temperatures of 25°C, 35°C, and 45°C.

Through Fig. 8, it can be observed that there was an increase in the concentration of ATZ solutions and there was a stabilization of the amount adsorbed. These results may be implicated in terms of limiting sites of the adsorbent sorption, which can have enough capacity to accommodate the increase of the number of molecules of ATZ available to be adsorbed on the MO seed surface [40].

Table 4 presented the data obtained by Langmuir and Freundlich isotherm models for the studied temperatures.

According to the results in Table 4, the experimental data were well explained by the two suggested models. As the seed is a complex and heterogeneous biomass, it is suggested that the Freundlich model may be more appropriate to explain how the ATZ biosorption occurs.

Freundlich isotherm model [41] assumes that the adsorbent surface is heterogeneous, which leads to a heterogeneous distribution of adsorption to the different locations of the material surface with different energies.

However, it is also believed that primarily ATZ interacts with the MO seed pores per monolayer, thus explaining the proper adjustment of the Langmuir model. Through Table 4, it can be observed that the value of equilibrium parameter of Langmuir isotherm ( $R_L$ ) is between 0 and 1, indicating that the adsorption is favorable. The results shows a significant sorption in low concentration [17].

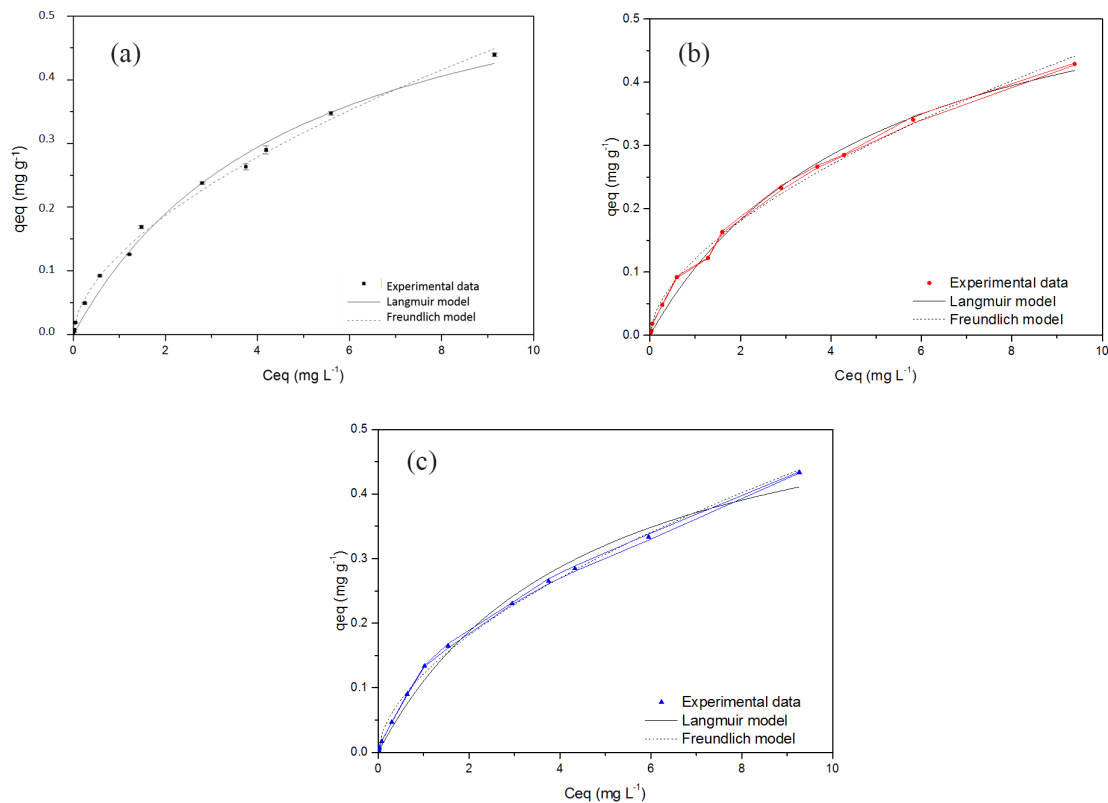


Fig. 8. Adjustment of Langmuir and Freundlich isotherm models to experimental data of atrazine sorption at temperatures: (a) 25°C, (b) 35°C, and (c) 45°C.

Table 4  
 Constants of Langmuir and Freundlich isotherm for the adsorption of atrazine in *Moringa oleifera* seeds

Temperature (°C)	Constant of Langmuir				Constant of Freundlich		
	$q_{eq} (mg\ g^{-1})$	$b_L (L\ mg^{-1})$	$R^2$	$R_L$	$n_F$	$k_F (mg\ g^{-1}\ L^{1/n}\ mg^{-1/n})$	$R^2$
25	0.653	0.205	0.992	0.198	0.576	0.125	0.996
35	0.643	0.198	0.994	0.204	0.578	0.121	0.996
45	0.613	0.219	0.991	0.188	0.574	0.122	0.995

According to Gupta et al. [42], the  $n_F$  value is known as Freundlich's factor of heterogeneity of the adsorbent and varies between 0 and 1; the closer to 0, the more heterogeneous the adsorbent surface is. This value indicated that the adsorption is favorable.

In the study of Almeida et al. [43], that evaluate MO seeds in the adsorption of Benzene, toluene, ethylbenzene and xylene compounds, the isotherm model of Freundlich better describe the adsorption of the substances in MO seeds. The authors have attributed that the BTEX adsorption process was influenced by the heterogeneity of the MO seed surface because there are active sites with different adsorptive energies.

### 3.5. Adsorption thermodynamics

Through the data obtained in Section 3.4, it is possible to calculate the energies involved in the ATZ biosorption process that are presented in Table 5.

The increase of the values of  $\Delta G^\circ$  in relation to the temperature increase point out that there is less motive power in the interaction between adsorbate and adsorbent and, therefore, resulting in lower adsorption capacity [44]. According to Zolgharnein et al. [2], for negative  $\Delta G^\circ$ , the process is considered thermodynamically spontaneous and favorable. For negative  $\Delta H$ , it is indicated that the nature of the ATZ adsorption process by MO seed is exothermic.

The physisorption mechanism energy of electrostatic interaction among adsorption and adsorbate sites is generally in the order from 2.0 to 20  $\text{kJ mol}^{-1}$  [44,45]. According to Hayward and Trapnell [46], the chemisorption energy is generally in the order of 80–200  $\text{kJ mol}^{-1}$ . Thus, these results show that the ATZ biosorption process is through physical adsorption. The value found of  $\Delta S$  points the probability of favorable adsorption without any structural change on the surface solid–liquid. The adsorption occurs in an orderly manner [47].

According to the results obtained, it can be verified that the MO seed has potential for ATZ biosorption. The literature presents some process for ATZ removal/degradation from water: ATZ degradation present in a suspension of  $\text{TiO}_2$ , using simulated solar radiation [48]; simultaneous oxidation of p-hydroxybenzoic acid and ATZ through the system of  $\text{Fe(III)/H}_2\text{O}$  [6]; the ATZ degradation by gamma rays irradiation [8]; ATZ removal using electrochemical advanced oxidation processes [49]; ATZ removal by combination of activated carbon and dielectric barrier discharge [50]; and ATZ biodegradation using moving bed biofilm reactor [51]. These methods are usually of high cost and high technological demand, and the adsorption is an alternative process of low cost, simple, and of easy application.

Table 5  
 Thermodynamic parameters of atrazine adsorption with *Moringa oleifera* Lam seed

Temperature (°C)	$\Delta G^\circ$ ( $\text{kJ mol}^{-1}$ )	$\Delta H$ ( $\text{kJ mol}^{-1}$ )	$\Delta S$ ( $\text{kJ mol}^{-1}\text{K}^{-1}$ )	$R^2$
25	-5.09	-21.76	-0.056	0.953
35	-4.26			
45	-3.98			

## 4. Conclusions

The MO seed presented as a potential adsorbent for the ATZ removal from aqueous solutions. The adsorption assays showed that the relevant parameters to the ATZ adsorption process by MO seed were the pH and dose of adsorbent.

The Lagergren kinetic model explained the experimental adsorption data, the kinetic equilibrium was reached in 20 min, and the ATZ removal of 76%. The adsorption data were adjusted to the isotherms Langmuir and Freundlich, and maximum capacity of sorption were calculated by obtaining a value of  $0.653\ \text{mg g}^{-1}$  and  $0.125\ \text{mg g}^{-1}\ \text{L}^{1/n}\ \text{mg}^{-1/n}$ , respectively, indicating that the adsorption is favorable. The negative thermodynamic values ( $\Delta G^\circ$ ,  $\Delta H$ , and  $\Delta S$ ) indicate that the sorption is favorable, spontaneous, and of exothermic nature, indicating that the physical adsorption process occurs.

Therefore, the MO seed would be used efficiently to remove ATZ from contaminated water, with a removal capacity varying from 50% to 90% depending on the initial concentration of ATZ. Once when the MO seed has not been previously subjected to a chemical or a physical treatment, it can be considered as an efficient alternative for organic contaminants removal.

## Acknowledgments

We thank the National Council for Scientific and Technological Development (CNPq), the Coordination for the Improvement of Higher Education Personnel (CAPES Foundation), and the Araucaria Foundation for financial support of this study.

## References

- [1] I. Ali, M. Asim, T.A. Khan, Low cost adsorbents for the removal of organic pollutants from wastewater, *J. Environ. Manage.*, 113 (2012) 170–183.
- [2] J. Zolgharnein, A. Shahmoradi, J. Ghasemi, Pesticides removal using conventional and low-cost adsorbents: a review, *Clean: Soil, Air, Water*, 39 (2011) 1105–1119.

- [3] J. Boucher, L. Steiner, I.W. Marison, Bio-sorption of atrazine in the press-cake from oilseeds, *Water Res.*, 41 (2007) 3209–3216.
- [4] L. Wu, H. Chang, X. Ma, A modified method for pesticide transport and fate in subsurface environment of a winter wheat field of Yangling, China, *Sci. Total Environ.*, 609 (2017) 385–395.
- [5] H. Chen, E. Bramanti, I. Longo, M. Onor, C. Ferrari, Oxidative decomposition of atrazine in water in the presence of hydrogen peroxide using an innovative microwave photochemical reactor, *J. Hazard. Mater.*, 186 (2011) 1808–1815.
- [6] M.P. Ormad, N. Miguel, A. Claver, J.M. Matesanz, J.L. Ovelheiro, Pesticides removal in the process of drinking water production, *Chemosphere*, 71 (2008) 97–106.
- [7] Z. Vryzas, G. Vassiliou, C. Alexoudis, E. Papadopoulou-Mourkidou, Spatial and temporal distribution of pesticide residues in surface waters in northeastern Greece, *Water Res.*, 43 (2009) 1–10.
- [8] J.A. Khan, N.S. Shah, S. Nawaz, M. Ismail, F. Rehman, H.M. Khan, Role of eq<sub>7</sub>, OH and H in radiolytic degradation of atrazine: a kinetic and mechanistic approach, *J. Hazard. Mater.*, 288 (2015) 147–157.
- [9] J. Boucher, L. Steiner, I. Marison, Bio-sorption of atrazine in the press-cake from oilseeds, *Water Res.*, 41 (2007) 3209–3216.
- [10] S. Shoukat, H.N. Bhatti, M. Iqbal, S. Noreen, Mango stone biocomposite preparation and application for crystal violet adsorption: a mechanistic study, *Microporous Mesoporous Mater.*, 239 (2017) 180–189.
- [11] H.N. Bhatti, A. Jabeen, M. Iqbal, S. Noreen, Z. Naseem, Adsorptive behavior of rice bran-based composites for malachite green dye: isotherm, kinetic and thermodynamic studies, *J. Mol. Liq.*, 237 (2017) 322–333.
- [12] Z. Aksu, Application of biosorption for the removal of organic pollutants: a review, *Process Biochem.*, 40 (2005) 997–1026.
- [13] S. Nausheen, H. Bhatti, M. Hanif, K.-U. Rehman, Enhanced removal of golden XGL dye by clay composites: batch and column studies, *Pol. J. Environ. Stud.*, 26 (2017) 2113–2123.
- [14] P.F. Coldebella, M.R. Fagundes-Klen, L. Nishi, K.C. Valverde, E.B. Cavalcanti, A. Dos Santos, O. Aparecida, R. Bergamasco, Potential effect of chemical and thermal treatment on the kinetics, equilibrium, and thermodynamic studies for atrazine biosorption by the *Moringa oleifera* pods, *Can. J. Chem. Eng.*, 95 (2017) 961–973.
- [15] F.K. Amagloh, A. Benang, Effectiveness of *Moringa oleifera* seed as coagulant for water purification, *Afr. J. Agric. Res.*, 4 (2009) 119–123.
- [16] J. Regalbutto, J. Robles, *The Engineering of Pt/Carbon Catalyst Preparation*, University of Illinois, Chicago, 2004.
- [17] M. Akhtar, S.M. Hasany, M.I. Bhangar, S. Iqbal, Sorption potential of *Moringa oleifera* pods for the removal of organic pollutants from aqueous solutions, *J. Hazard. Mater.*, 141 (2007) 546–556.
- [18] S. Lagergren, Zur Theorie der sogenannten Absorption gelöster Stoffe, P.A. Norstedt & Söner, Stockholm, 1898.
- [19] Y.-S. Ho, G. McKay, Kinetic models for the sorption of dye from aqueous solution by wood, *Process Saf. Environ. Prot.*, 76 (1998) 183–191.
- [20] I. Langmuir, The adsorption of gases on plane surfaces of glass, mica and platinum, *J. Am. Chem. Soc.*, 40 (1918) 1361–1403.
- [21] H. Freundlich, Over the adsorption in solution, *J. Phys. Chem.*, 57 (1906) 1100–1107.
- [22] D.H.K. Reddy, K. Seshiah, A. Reddy, S. Lee, Optimization of Cd (II), Cu (II) and Ni (II) biosorption by chemically modified *Moringa oleifera* leaves powder, *Carbohydr. Polym.*, 88 (2012) 1077–1086.
- [23] Y. Liu, Is the free energy change of adsorption correctly calculated?, *J. Chem. Eng. Data*, 54 (2009) 1981–1985.
- [24] F.B. Scheufler, A.N. Módenes, C.E. Borba, C. Ribeiro, F.R. Espinoza-Quiñones, R. Bergamasco, N.C. Pereira, Monolayer-multilayer adsorption phenomenological model: kinetics, equilibrium and thermodynamics, *Chem. Eng. J.*, 284 (2016) 1328–1341.
- [25] V.N. Alves, R. Mosquetta, N.M.M. Coelho, J.N. Bianchin, K.C.D.P. Roux, E. Martendal, E. Carasek, Determination of cadmium in alcohol fuel using *Moringa oleifera* seeds as a biosorbent in an on-line system coupled to FAAS, *Talanta*, 80 (2010) 1133–1138.
- [26] C.S. Araújo, D.C. Carvalho, H.C. Rezende, I.L. Almeida, L.M. Coelho, N.M. Coelho, T.L. Marques, V.N. Alves, Bioremediation of Waters Contaminated with Heavy Metals Using *Moringa oleifera* Seeds as Biosorbent, InTech, Croatia, 2013.
- [27] Y. Wang, H. Gao, R. Yeredla, H. Xu, M. Abrecht, Control of pertechnetate sorption on activated carbon by surface functional groups, *J. Colloid Interface Sci.*, 305 (2007) 209–217.
- [28] M.T. Uddin, M.A. Islam, S. Mahmud, M. Rukanuzzaman, Adsorptive removal of methylene blue by tea waste, *J. Hazard. Mater.*, 164 (2009) 53–60.
- [29] V. Boonamnuayvitaya, S. Sae-Ung, W. Tanthapanichakoon, Preparation of activated carbons from coffee residue for the adsorption of formaldehyde, *Sep. Purif. Technol.*, 42 (2005) 159–168.
- [30] N.B. Colthup, Spectra-structure correlations in the infra-red region, *J. Opt. Soc. Am.*, 40 (1950) 397–400.
- [31] M.F. Silva, E.A.G. Pineda, A.A.W. Hechenleitner, D.M. Fernandes, M.K. Lima, P.R.S. Bittencourt, Characterization of poly(vinyl acetate)/sugar cane bagasse lignin blends and their photochemical degradation, *J. Therm. Anal. Calorim.*, 106 (2011) 407–413.
- [32] R.D.C.A. Javaroni, M.D. Landgraf, M.O.O. Rezende, Comportamento dos herbicidas atrazina e alaclor aplicados em solo preparado para o cultivo de cana-de-açúcar, *Quim. Nova*, 22 (1999) 58–64.
- [33] C. Bellmann, A. Caspari, V. Albrecht, T.L. Doan, E. Mäder, T. Luxbacher, R. Kohl, Electrokinetic properties of natural fibres, *Colloids Surf., A*, 267 (2005) 19–23.
- [34] J.B. Weber, Interaction of organic pesticides with particulate matter in aquatic and soil systems, *Adv. Chem.*, 111 (1972) 55–120.
- [35] S.O. Lesmana, N. Febriana, F.E. Soetaredjo, J. Sunarso, S. Ismadji, Studies on potential applications of biomass for the separation of heavy metals from water and wastewater, *Biochem. Eng. J.*, 44 (2009) 19–41.
- [36] L.G. Morrill, B.C. Mahilum, S.H. Mohiuddin, *Organic compounds in soils: sorption, degradation and persistence*, Ann Arbor Science Publishers, Inc., Ann Arbor, Michigan, 1982.
- [37] R.M. Behki, S.U. Khan, Degradation of atrazine, propazine, and simazine by Rhodococcus strain B-30, *J. Agric. Food Chem.*, 42 (1994) 1237–1241.
- [38] S. Raghuvanshi, R. Singh, C. Kaushik, A. Raghav, Kinetics study of methylene blue dye bioadsorption on bagasse, *Appl. Ecol. Environ. Res.*, 2 (2004) 35–43.
- [39] E. Ayranci, N. Hoda, Adsorption kinetics and isotherms of pesticides onto activated carbon-cloth, *Chemosphere*, 60 (2005) 1600–1607.
- [40] M. Akhtar, M. Bhangar, S. Iqbal, S.M. Hasany, Efficiency of rice bran for the removal of selected organics from water: kinetic and thermodynamic investigations, *J. Agric. Food Chem.*, 53 (2005) 8655–8662.
- [41] H. Freundlich, Over the adsorption in solution, *J. Phys. Chem.*, 57 (1906) 85.
- [42] V. Gupta, B. Gupta, A. Rastogi, S. Agarwal, A. Nayak, Pesticides removal from waste water by activated carbon prepared from waste rubber tire, *Water Res.*, 45 (2011) 4047–4055.
- [43] I.L.S. Almeida, N.R.A. Filho, M.I.R. Alves, B.G. Carvalho, N.M.M. Coelho, Removal of BTEX from aqueous solution using *Moringa oleifera* seed cake, *Environ. Technol.*, 33 (2012) 1299–1305.
- [44] Y. Ho, J. Porter, G. McKay, Equilibrium isotherm studies for the sorption of divalent metal ions onto peat: copper, nickel and lead single component systems, *Water Air Soil Pollut.*, 141 (2002) 1–33.
- [45] R.C. Bansal, M. Goyal, *Activated Carbon Adsorption*, CRC press, New York, 2005.
- [46] D.O. Hayward, B.M.W. Trapnell, *Chemisorption*, Butterworths London, 1964.
- [47] M. Akhtar, S.M. Hasany, M. Bhangar, S. Iqbal, Low cost sorbents for the removal of methyl parathion pesticide from aqueous solutions, *Chemosphere*, 66 (2007) 1829–1838.

- [48] T. Aungpradit, P. Sutthivaiyakit, D. Martens, S. Sutthivaiyakit, A.A.F. Kettrup, Photocatalytic degradation of triazophos in aqueous titanium dioxide suspension: identification of intermediates and degradation pathways, *J. Hazard. Mater.*, 146 (2007) 204–213.
- [49] S. Komtchou, A. Dirany, P. Drogui, D. Robert, P. Lafrance, Removal of atrazine and its by-products from water using electrochemical advanced oxidation processes, *Water Res.*, 125 (2017) 91–103.
- [50] P. Vanraes, G. Willems, A. Nikiforov, P. Surmont, F. Lynen, J. Vandamme, J. Van Durme, Y.P. Verheust, S.W.H. Van Hulle, A. Dumoulin, C. Leys, Removal of atrazine in water by combination of activated carbon and dielectric barrier discharge, *J. Hazard. Mater.*, 299 (2015) 647–655.
- [51] Z. Derakhshan, M.H. Ehrampoush, A.H. Mahvi, M.T. Ghaneian, S.M. Mazloomi, M. Faramarzian, M. Dehghani, H. Fallahzadeh, S. Yousefinejad, E. Berizi, S. Bahrami, Biodegradation of atrazine from wastewater using moving bed biofilm reactor under nitrate-reducing conditions: a kinetic study, *J. Environ. Manage.*, 212 (2018) 506–513.